Time-Resolved Mass Spectrometry of Nano-Al and Nano-Al/CuO Thermite under Rapid Heating: A Mechanistic Study
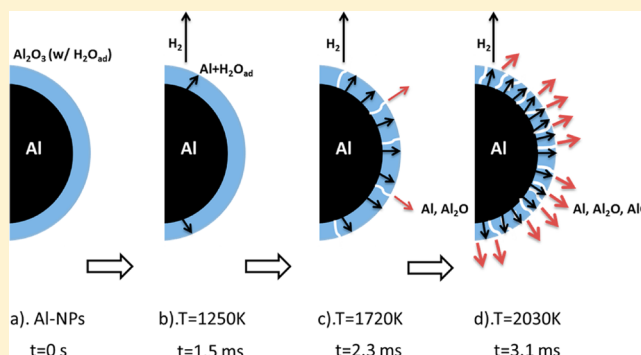
Guoqiang Jian,[†] Nicholas W. Piekiel,[‡] and Michael R. Zachariah*,[†,‡]

[†]Department of Chemistry and Biochemistry, University of Maryland, College Park, Maryland 20742, United States
[‡]Department of Mechanical Engineering, University of Maryland, College Park, Maryland 20742, United States

S *Supporting Information*

ABSTRACT: Aluminum nanoparticles (Al-NPs) and nano-Al/CuO thermite were investigated in a rapid heating environment by temperature jump time-of-flight mass spectrometry. Upon rapid heating (10^5 to 10^6 K/s), Al-containing vapor species (Al and Al_2O) are observed to slowly increase with increasing temperature, followed by a rapid increase in concentration at ~2030 K. The temporal evolution of Al, Al_2O species observed in time-resolved mass spectra of rapid heated Al-NPs supports the hypothesis that Al containing species diffuse outward through the oxide shell under high heating rate conditions. The rapid rise in Al-containing species above 2030 K, which is below the bulk melting point of Al_2O_3, implies that the penetration of Al into the shell probably decreases its melting point. The measurements lead to an effective overall diffusion coefficient of ~10^{-10} cm²/s. Time-resolved mass spectra of nano-Al/CuO thermite show for the first time the existence of Al, Al_2O, AlO, and Al_2O_2 intermediate reaction products, with Al_2O the main intermediate oxidation product, in agreement with thermochemical calculations.

a). Al-NPs t=0 s
b).T=1250K t=1.5 ms
c).T=1720K t=2.3 ms
d).T=2030K t=3.1 ms

1. INTRODUCTION

The nanothermite reaction is a highly exothermic reaction between metal fuel and oxidizer particles at the nanoscale. Aluminum nanoparticles (Al-NPs) are the most commonly used fuel due to their ready availability, high energy density, and reactivity.[1−3] It is well-known that a 2−5 nm thick oxide (typically amorphous Al_2O_3) coating is present on the surface of Al-NPs, which prevents the further oxidation of the metal at low temperature.[4,5] In this regard, nano-aluminum can be considered as a core−shell nanoparticle with the oxide shell comprising a significant fraction of the particle mass, exceeding 50% in some cases.[6]

The ignition of aluminum particles has been found to be very sensitive to particle size and closely related to the properties of the oxide shell. It has been found that Al-NPs can be ignited at as low as ~930 K which is close to the melting point of the Al (933 K). The microsized aluminum particles ignite at a much higher temperature of ~2300 K that is close to the melting point of the oxide shell.[7] Two mechanisms have been proposed to explain initiation/oxidation of Al-NPs. The first mechanism may be broadly classified as a diffusion based phenomenon where Al and oxygen species diffuse through the oxide shell.[8,9] The second alternative mechanism, the so-called "melt-dispersion mechanism", suggests that the aluminum core expands and ruptures the oxide shell at high heating rates, resulting in ejection of small molten clusters of aluminum at high velocities.[10−12] In melt-dispersion, mechanical breakdown

of the aluminum oxide shell occurs at temperatures much lower than the melting point of the aluminum oxide shell, and plays an important role in the ignition of Al-NPs.[11] These two mechanisms offer radically different views of how nano-aluminum ignition is initiated.

In this paper, a temperature-jump time-of-flight mass spectrometer (T-Jump/TOFMS) was used to investigate the product speciation from Al-NPs and nano-Al/CuO thermite under rapid heating ($10^5−10^6$ K/s). Transmission electron microscopy (TEM) was used to characterize the morphological evolution of the Al-NPs, for which in some cases we found hollow structures in the heated Al-NPs. Our results indicate that aluminum core atoms diffuse outward through the oxide shell during the rapid heating.

2. EXPERIMENTAL SECTION

2.1. Sample Preparation. Al-NPs purchased from Argonide Corporation (50 nm ALEX powder) are used in this study. The Al-NPs were found to contain ~70% active Al by mass, as determined by TGA, due to the aluminum oxide shell. Copper oxide (CuO) nanoparticles are purchased from Sigma-Aldrich, and specified by the supplier to be <50 nm. Al_2O_3 particles are also purchased from Sigma-Aldrich, with a
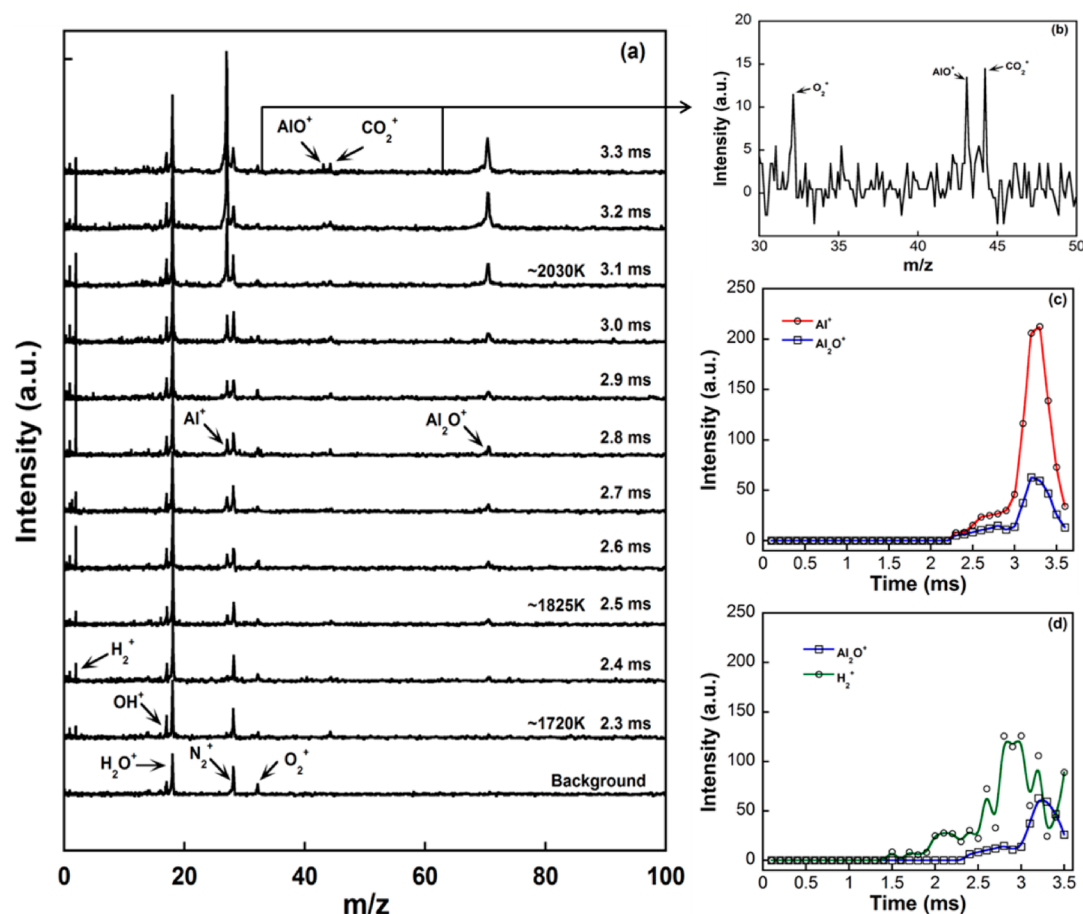
Figure 1. (a) Time-resolved mass spectra obtained from rapid heated Al-NPs on iridium wire, (b) the zoom-in view of the mass spectrum at t = 3.3 ms, (c) typical results of Al^+ and Al_2O^+ ion species, and (d) H_2^+ and Al_2O^+ ion species during rapid heating.

purity of ≥98%. For sample preparation, Al-NPs, Al_2O_3 particles, and nano-Al/CuO were ultrasonicated in hexane for 20 min, and then coated onto the T-Jump probe with a micropipet.

2.2. T-Jump/TOFMS. The details of the T-Jump/TOFMS and operational setting can be found in our previous papers.[13,14] Typically, the T-Jump probe in this study is an ~12 mm long, 76 μm diameter platinum or iridium wire. In previous studies, the T-Jump system used a platinum filament that limited the heating temperature to around ~1800 K. In the present study, we also employ an iridium wire capable of temperatures in excess of 2000 K. A small portion of the central region (3−4 mm) of the wire is coated with the solid sample, and inserted into the vacuum chamber of the mass spectrometer, near the electron ionization region. The electron beam is normally operated at 70 eV and 1 mA, with the background pressure in the TOF chamber at ~4.2 × 10^{-6} Torr. The T-Jump probe can be heated by an in-house built power source at a rate of up to ~10^6 K/s. From the current and voltage trace, a resistivity measurement can be obtained and related to the instantaneous temperature of the platinum[15] or iridium wire,[16] which can be mapped against the mass spectra. The sample temperature is estimated to be ~5 K less than that of the wire temperature based on simulation results.[9] Time-resolved mass spectra combined with temperature information can be obtained and used for the characterization of the species produced during the rapid heating. The T-Jump mass spectrometer is also enabled with an optical port to enable

simultaneous high speed imaging using a Phantom v12.0 digital camera (67 065 frames per second). This enables then the simultaneous temporal characterization of the temperature, species, and visible combustion dynamics.

3. RESULTS

3.1. Rapidly Heated Nano-Aluminum in T-Jump/TOFMS. In our previous T-Jump system, we used a platinum wire which limited the heating temperature to around ~1800 K, which is below the melting point of alumina. To address this limitation, we also employ an iridium wire which allows us to probe higher temperatures (>2000 K). We begin our analysis with the neat Al-NPs (without oxidizer), which were pulse heated to 2030 K in 3.1 ms in the TOFMS, at a heating rate of ~6 × 10^5 K/s. During heating, a sequence of 95 spectra with mass to charge ratio (m/z) up to 380 were recorded at 100 μs intervals. We plot the mass spectra between t = 2.3 and 3.3 ms in Figure 1a. Although we sampled up to m/z ~380, no high-mass ions were observed and major ions were only seen for m/z < 100. Background species of the spectrometer consist of H_2O^+, OH^+, N_2^+, and O_2^+. Upon heating, we observe Al^+, Al_2O^+, AlO^+ (zoom-in view shown in Figure 1b), and H_2^+ product species, and an increased intensity of H_2O^+. The major aluminum containing species observed are Al^+ and Al_2O^+, which we plot temporally in Figure 1c. Both Al^+ and Al_2O^+ appear simultaneously at t = 2.3 ms, which corresponds to a wire temperature of 1720 K, and peaks at t = 3.1 ms (T = 2030 K). This is one of the key results of this paper which we will

interpret. Typical results of H_2^+ and Al_2O^+ species during the rapid heating are also plotted and shown in Figure 1d. A similar rapid heating experiment was also run for Al_2O_3 particles (Sigma-Aldrich, ≥98%), which were rapidly heated to 2070 K in 3 ms. The experiment yielded no observable Al_2O. The known ionization cross sections (σ) for different Al containing species[17] are used for the estimation of their partial pressure (p) (i.e., concentrations) from the measured ion intensities ($I \propto p \times \sigma$), to enable comparison of the concentrations of different species. The ionization cross section data for Al, Al_2O, AlO, and Al_2O_2 are summarized in Table 1.[18−20]

Table 1. Electron Impact Ionization Cross Section of Al, Al_2O, AlO, and Al_2O_2 at 70 eV[18−20]

species	Al	Al_2O	AlO	Al_2O_2
σ (Å²)	7.5	11.8	4.8	6.0

To study the effect of the heating rate, we changed the heating pulse to ~2 and 5 ms, which correspond to a heating rate of ~9×10^5 and 3×10^5 K/s, respectively. In these runs, we observe Al^+ appearance at 1825 and 1705 K, respectively. Similar to the 3 ms heating pulse, we also observe H_2 produced at ~1250 K, as well as an increased intensity of H_2O upon rapid heating.

To further investigate the possibility that at lower temperatures elemental aluminum is reacting with adsorbed water, we measured the evolution of hydrogen production, which is shown in Figure 2. We rapidly heated the Al-NPs to 1650 K at a
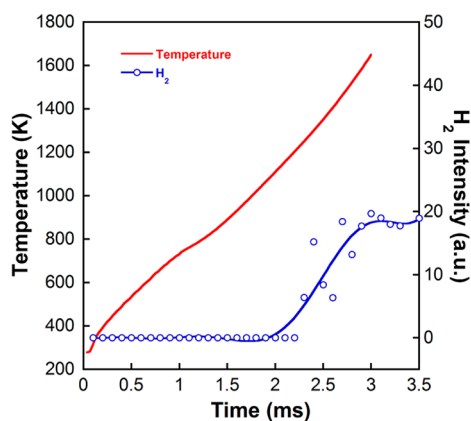
Figure 2. Temporal evolution of hydrogen peak intensity of rapid heating of Al-NPs up to 1650 K in 3 ms.

heating rate of ~5×10^5 K/s and observe H_2^+ onset at $t = 2.3$ ms, corresponding to a temperature of ~1250 K. This implies that significant aluminum diffusion is occurring and possibly reacting with adsorbed water in the alumina shell, which we will discuss further later. The TEM images of the heated Al-NPs (up to 1650 K in 3 ms) are shown in Figure 3. Many of the particles appear unchanged after rapid heating; however, a few are seen to be hollow, implying that aluminum can diffuse out of the shell without a catastrophic change in the shell structure. A similar hollow structure was also reported in Al-NP oxidation at high temperatures by Rai et al.[8]

3.2. Nano-Aluminum/CuO Thermite Reaction in T-Jump/TOMFS. A more vigorous reaction of nano-Al was probed with a thermite mixture using CuO as the oxidizer at a heating rate of ~5×10^5 K/s. To better study the intermediate
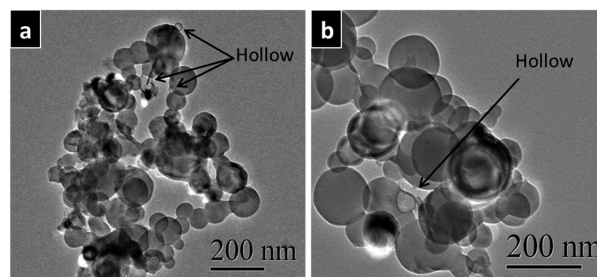
Figure 3. TEM images of Al-NPs after rapid heating up to 1650 K.

reaction species during the thermite reactions, especially those related to Al species, fuel rich (equivalence ratio $\phi = 3$) nano-Al/CuO thermites were probed. The T-Jump mass spectrometer probe has been implemented with an optical port to enable simultaneous high speed imaging using a Phantom v12.0 digital camera. Figure 4 shows sequential snapshots of fuel rich nano-

Figure 4. Selected images for a fuel rich nano-Al/CuO reaction recorded by a high-speed digital camera.

Al/CuO ignited on the Pt wire at a heating rate of ~5×10^5 K/s. It is seen from Figure 4 that the optical signal is first observed at the two ends of the sample coating at a time of 1.446 ms (~1000 K), indicating the ignition of the thermite sample. The ignition front then propagates from the two ends toward the center and ignites the whole thermite sample at a time of 1.535 ms. Time-resolved mass spectra for the reaction are shown in Figure 5. The mass spectra in Figure 5 clearly show the thermite reaction progression and intermediate reaction species, which corresponds to the high speed imaging in
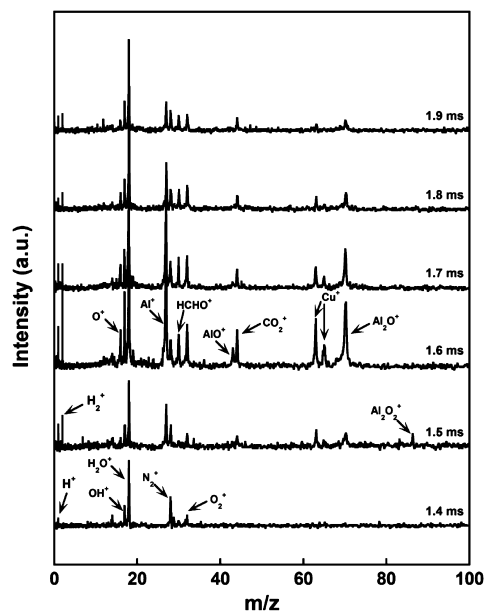
Figure 5. Time-resolved mass spectra obtained from a fuel rich nano-Al/CuO thermite reaction.

Figure 4. In Figure 6, we plot the time dependent evolution of different species from fuel rich nano-Al/CuO thermite reaction,
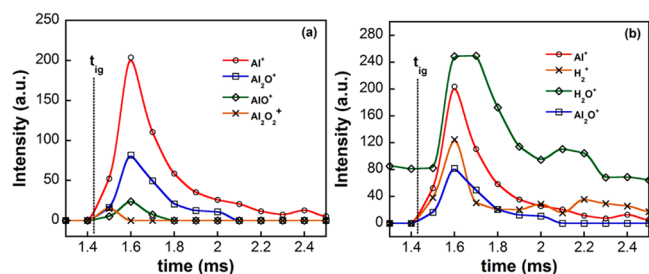

Figure 6. Time dependent evolution of (a) Al^+, Al_2O^+, AlO^+, and $Al_2O_2^+$ and (b) Al^+, Al_2O^+, H_2O^+, and H_2^+ from a fuel rich nano-Al/CuO thermite reaction.

to be discussed later. From the time-resolved mass spectra shown in Figure 5, we can see Al at ~1.5 ms (~1015 K). At later times, we see the strongest intermediate ion peaks, which include Al^+, $Al_2O_2^+$, AlO^+, $Al_2O_2^+$, O_2^+, Cu^+, H_2^+, and some carbon containing species of CH_2O^+ and CO_2^+. Cu^+ is a product from the Al/CuO thermite reaction, while O_2^+ is from the thermal decomposition of the CuO nanoparticles.[21] Similar to the rapid heating of Al NPs, we also observed a strong H_2^+ peak, presumably from the reaction between the outward radially diffused Al and adsorbed water in the shell. Carbon containing species are likely from the decomposition of the thin layer of $CuCO_3$ on the surface CuO nanoparticles[21] and/or hydrocarbon formed on the surface of CuO nanoparticles during the sonication in hexane.

3.3. Calculated Equilibrium Mole Fraction of Alumina Decomposition and Thermite Reaction at High Temperature. Thermodynamic equilibrium mole fractions of Al_2O and AlO products for pure alumina decomposition as well as 30 wt % Al_2O_3 + 70 wt % Al (similar mass ratio to Al NPs) at high temperatures of 1900−2000 K are shown in Table 2 using

Table 2. Thermodynamic Equilibrium Mole Fraction of Al_2O and AlO Products Using NASA CEA Code for Aluminum Oxide Decomposition[a]

starting materials	species	T = 1900 K	T = 1950 K	T = 2000 K
pure Al_2O_3	Al_2O	2.19×10^{-3}	4.2×10^{-4}	8×10^{-5}
	AlO	2.691×10^{-2}	1.209×10^{-2}	5.53×10^{-3}
30 wt % Al_2O_3 + 70 wt % Al	Al_2O	3.10×10^{-3}	5.8×10^{-4}	1.2×10^{-4}
	AlO	1.873×10^{-2}	8.51×10^{-3}	3.91×10^{-3}

[a]Constant pressure and constant temperature thermochemical calculation. $P = 10^{-9}$ atm.

NASA CEA code. From Table 2, it shows that only a small fraction of Al_2O and AlO exist for both cases. Moreover, AlO mole fraction is always higher than Al_2O species at high temperatures from 1900 to 2000 K.

Thermochemical equilibrium calculation results from the NASA CEA code for fuel rich Al/CuO thermites ($\phi = 3$) are shown in Figure 7 at pressures of 10^{-4} and 1 atm. As shown in Figure 7, Al, Al_2O, AlO, and Al_2O_2 are the main product species predicted by thermodynamic calculations, in agreement with what we observed in the fuel rich nano-Al/CuO thermite reaction shown in Figure 5. From Figure 7, the species mole fractions predicted by thermochemical equilibrium calculation
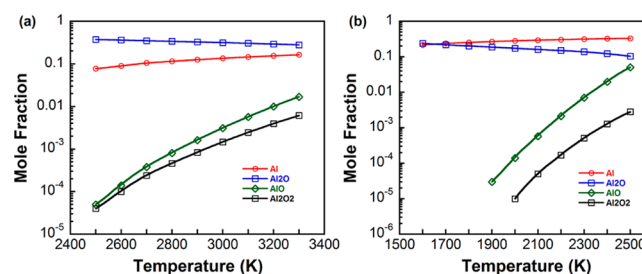

Figure 7. Calculated equilibrium mole fraction of major Al-containing species of fuel rich Al/CuO (phi = 3) using NASA CEA code. Pressure: (a) 1 atm and (b) 10^{-4} atm (considering 30% Al_2O_3 in Al NPs by mass).

results follow the order of Al_2O > AlO > Al_2O_2, which is consistent with mass spectrometry results of nano-Al/CuO thermite reaction in section 3.2.

4. DISCUSSION

4.1. Rapid Heating of Nano-Aluminum in Vacuum and Diffusion Based Mechanism. Heating of the Al-NPs to the melting point of Al should in the absence of any constraint from the shell result in a volumetric expansion ($\rho_{Al(l)}$ = 2.38 g/cm^3, $\rho_{Al(s)}$ = 2.70 g/cm^3). Since the thermal expansion coefficient of aluminum is much larger than that of alumina (the linear coefficient of aluminum being approximately 4 times that of alumina), it is expected that melted Al will be driven outward through the shell, or possibly rupture the shell. Nevertheless, we see no Al in the spectra (Figure 1a) until ~1720 K, and thus well above the melting point of elemental aluminum. One possibility for the lack of aluminum in the spectrum at temperatures above its melting point is that the aluminum diffusion does not produce a high enough signal for detection by the TOFMS. However, from prior work, it is well-known that the ignition temperature of nano-aluminum is well below this temperature. Another possibility is that we are observing Al containing species from the direct heating of the alumina shell. However, thermodynamic calculations (NASA CEA code) in Table 2 show that, if that were the case, (a) we should see less AlO_2 species with increasing temperature above 1900 K and (b) the concentration of AlO should be higher than Al_2O. In fact, we see the opposite effect with ~2.2 times higher concentration of Al_2O (see calculation steps in the Supporting Information). A more likely explanation for lack of aluminum at lower temperatures is that aluminum diffusing through the shell is reacting with adsorbed water in the alumina shell to produce hydrogen, which we do observe in the mass spectra at 1.5 ms (~1250 K). This point will be discussed later in this part. The absence of any higher order clusters of either Al or AlO_x implies that at least up to 2030 K no catastrophic mechanical breakdown of the aluminum oxide shell has occurred. A previous in situ high heating rate TEM experiment shows that aluminum oxide shell cracking can be seen, but no particle "spallating" was found after rapid heating to 1473 K in 1 ms, indicating that the aluminum core migrated outward through the shell during the heating.[22]

Recent reactive molecular dynamics (MD) simulation results by Chakraborty and Zachariah suggest that the diffusion of core Al ions into the shell changes the aluminum oxide structure into the aluminum rich metastable suboxide shell, which can melt at a temperature considerably lower than the melting point of aluminum oxide.[23] The sudden increase in the
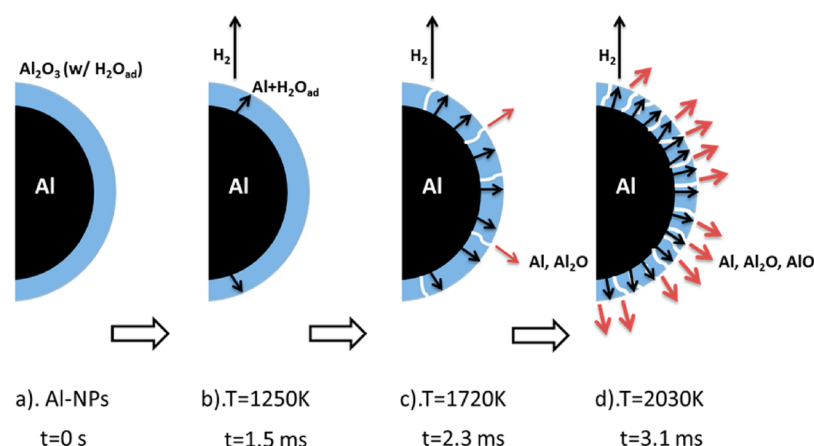
Figure 8. Schematics illustrate the rapid heating of the Al-NPs in a vacuum. (a) Initial Al-NPs with Al core-Al_2O_3 shell structure and adsorbed water in alumina shell. (b) Upon heating to the Al melting point, Al species start to diffuse outward and react with adsorbed water to produce H_2. (c) At T = 1720 K, more Al species diffuse/migrate outward and start to appear in mass spectra. (d) At T = 2030 K, the shell changes to suboxide and melts, more Al and Al_2O diffuse/migrate outward and AlO starts to appear in mass spectra.

aluminum peak at 2030 K suggests the shell is now melting, some 350 K below the reported alumina melting point, and results in a rapid increase in the rate of aluminum transport.

Our observations of H_2 under rapid heating of Al-NPs suggest a reaction between Al and H_2O which can produce H_2 ($Al + 3H_2O = Al(OH)_3 + 3/2H_2$) and an increase of H_2O upon heating Al-NPs. In fact, Navrotsky et al. have reported on water adsorption in nanoscale alumina.[24] They found that up to 3% (by weight) of adsorbed water exists in both α-Al_2O_3 and λ-Al_2O_3 alumina, and residual water (e.g., 0.48% weight for λ-Al_2O_3 with a surface area of 161 m^2/g) still exists even after heating the sample in a vacuum at 1023 K for 2 h. Hence, we conclude that the increase in water intensity in the mass spectra should be from desorption of adsorbed water in the alumina shell.
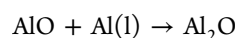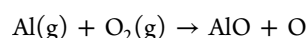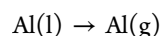
Considering the above, we propose a diffusion based mechanism that Al containing species diffuse outward through the oxide shell of Al-NPs under rapid heating shown schematically in Figure 8. A typical aluminum nanoparticle is shown in Figure 8a with aluminum core, alumina shell, and some absorbed water within the shell. Initially, the Al core melts upon rapid heating and diffuses outward through the shell, and reacts with the adsorbed water in the shell to produce hydrogen (Figure 8b). Hydrogen is observed when the Al-NPs are heated to ~1250 K. Higher temperatures will enhance the aluminum ion mobility through the oxide shell, which can be further enhanced by stress induced cracking or thinning of the oxide shell[22,25] and the built-in electric field induced by the oxide shell.[26] By 1720 K, Al and Al_2O species are observed (Figure 8c), and above T = 1720 K, more Al and Al_2O species migrate outward but show a slow increase in mass spectra. With the increasing aluminum ion diffusion through the shell and counter-diffusion of oxygen anion radially inward, the shell region thickens and leads to the formation of an aluminum rich suboxide shell. This suboxide as we have shown through molecular dynamics simulation[23] has a lower melting point than pure alumina, resulting in a much enhanced transport of aluminum. At this point, ~2030 K (Figure 8d), both Al and Al_2O show a significant increase and the appearance of AlO is also seen. On the basis of the proposed mechanism, we make a rough estimate of the effective diffusion coefficient $D = L^2/t_{delay}$ ~10^{-10} cm^2/s, where L = shell thickness and t_{delay} = the time

difference between the melting point of the aluminum, as determined by the wire temperature, and the time when we observe the first appearance of aluminum in the mass spectrometer.

The lack of any observed small clusters of aluminum or aluminum oxides as well as no catastrophic mechanical breakdown of the aluminum oxide shell below 2030 K suggest a diffusion process in our T-Jump rapid heating experiment of the Al-NPs.

4.2. Al-Containing Species in Rapid Heating of Al-NPs and Nano-Al/CuO Thermite Reaction. Many intermediate reaction products have been found or suggested in the oxidation of the aluminum through experiments,[27−32] thermodynamic calculation,[33] and molecular simulation,[34,35] but only AlO has been experimentally observed by in situ optical absorption/emission spectrum. By contrast, AlO, Al_2O, and Al_2O_2 are predicted to be the main intermediate oxidation reaction products by thermodynamic calculation[33] and MD simulation.[34] In part, the difference between observation and prediction is due to the limitations of available optical transitions of the optical methods which are limited to detecting Al and AlO. The mass spectrometry method has no constraints on species type, and as shown in Figure 1a, we find Al and Al_2O as the main product species of the rapidly heated Al-NPs. A small peak of AlO^+ was found to appear at t = 3.1 ms (2030 K), and a typical zoom in spectra with AlO^+ is shown in Figure 1b. Thus, in contrast to optical measurements, we expect Al_2O as the main intermediate oxidation product based on its existence as a major intermediate species of rapidly heated Al-NPs.

Yuasa et al. have proposed the following mechanism for Al_2O formation:[27]

$$Al(l) \rightarrow Al(g)$$

$$Al(g) + O_2(g) \rightarrow AlO + O$$

$$Al(g) + O + M \rightarrow AlO + M$$

$$AlO + Al(l) \rightarrow Al_2O$$

This mechanism suggests that the AlO and Al are precursors of the Al_2O. This mechanism was developed for the burning of micrometer sized aluminum in a droplet burning or diffusion

flame configuration. Nanoparticles will burn much differently,[32] and typically by surface reaction processes. Moreover, unlike the mechanism above, our O_2 concentration, as observed in Figure 1, is too small to account for Al_2O production (i.e., $Al_2O \gg O_2$). The mechanism above implies that Al_2O is formed from an AlO precursor, which we find occurs in very low to nonmeasurable concentrations. Our results imply that Al_2O is formed directly from the surface without volatilization of AlO.

One might expect that existence of adsorbed H_2O could contribute to the production of AlO_x; however, H_2^+ and Al_2O^+ peaks in Figure 1d do not follow the same trend with increasing temperature, indicating that Al_2O is not coming from direct reaction of diffused Al and adsorbed H_2O in the shell. To determine if the origin of the Al_2O species could be attributed to the decomposition of the rapidly heated alumina shell, Al_2O_3 particles (Sigma-Aldrich, $\geq 98\%$) were rapidly heated to 2070 K in 3 ms and the experiment yielded no observable Al_2O. Moreover, Puri and Yang's simulation results have shown Al-containing fragments from 5 nm alumina particles when heated beyond 4000 K.[36] Thus, we may conclude that the observed Al_2O cannot be attributed to dissociation or decomposition of the oxide shell, and must involve the migration of the aluminum core atoms.

MD simulations of rapid heating Al-NPs in a vacuum by Chakraborty and Zachariah have shown that Al from the core can diffuse into the shell and react with oxygen in the shell to form a metastable suboxide with lower O to Al ratio.[23] Similar results were also reported by Wang et al.[37] As the Al^+ and Al_2O^+ appear almost simultaneously and the intensity behaves similarly upon heating, as shown in Figure 1c, we can speculate that Al_2O might come from the reaction between diffused Al core and oxygen in the shell rather than from the dissociation of the oxide shell.

Given its existence as a major intermediate species in rapidly heated Al-NPs, we expect Al_2O as one of the main intermediate oxidation products of aluminum oxidation. As shown in Figures 5 and 6a, Al^+, Al_2O^+, AlO^+, and $Al_2O_2^+$ species predicted by thermochemical calculations appear after the ignition point and Al^+ and Al_2O^+ are the main species similar to those seen for rapid heating of Al-NPs. In fact, Al^+ and Al_2O^+ species were also observed in our previous time-resolved mass spectrometry study of stoichiometry nano-Al/CuO.[9,21] Time dependent species evolutions show that Al^+, Al_2O^+, and AlO^+ follow the same trend, while $Al_2O_2^+$ peaks earlier than other aluminum species. The earlier appearance and quick decreasing of the $Al_2O_2^+$ peak may indicate that Al_2O_2 decomposition contributes to the formation of AlO species, which has been previously proposed by Huang et al.[7]

Notice that, similar to the mass spectra of rapidly heated Al-NPs, only elemental Al is observed in the mass spectra shown in Figure 5, and no high order Al and AlO_x clusters are observed. Also, the high concentration of H_2^+ shown in Figure 5 further supports the existence of the adsorbed water. Figure 6b again shows that H_2^+ is produced by the reaction between Al and adsorbed water, which can be seen after the Al/CuO thermite reaction begins. The above results further support a diffusive mechanism in nanothermite reactions.

While prior works[28,29,32,33] have shown Al and AlO species, to our knowledge, this is the first experimental evidence of the existence of these four aluminum species during aluminum combustion and nanoparticle oxidation process.

5. CONCLUSIONS

In conclusion, we have used T-Jump/TOFMS to investigate Al-NPs and nano-Al/CuO thermite reactions at high heating rates of $\sim 10^5 - 10^6$ K/s. Time-resolved mass spectra were obtained for rapid heating of Al-NPs and fuel rich nano-Al/CuO thermite mixtures in which for the first time four Al-containing intermediate species have been observed (Al, Al_2O, AlO, Al_2O_2). Temporal evolution of Al, Al_2O, and H_2 species observed in time-resolved mass spectra of rapid heated Al-NPs supports the hypothesis that Al containing species diffuse outward through the oxide shell under high heating rate conditions.

■ ASSOCIATED CONTENT

Ⓢ Supporting Information

Results for the temporal evolution of water from rapid heating of Al-NPs up to ~ 2000 K, the temporal evolution of H_2O^+, OH^+, and H_2^+ under rapid heating of Al-NPs up to 1650 K in 3 ms, comparison of Al_2O and AlO species concentration in TOFMS, and estimation of background water flux in TOFMS. This material is available free of charge via the Internet at http://pubs.acs.org.

■ AUTHOR INFORMATION

Corresponding Author

*E-mail: mrz@umd.edu. Phone: 301-405-4311. Fax: 301-314-947.

Notes

The authors declare no competing financial interest.

■ ACKNOWLEDGMENTS

■ REFERENCES

(1) Yetter, R. A.; Risha, G. A.; Son, S. F. *Proc. Combust. Inst.* **2009**, *32*, 1819−1838.

(2) Dreizin, E. L. *Prog. Energy Combust. Sci.* **2009**, *35*, 141−167.

(3) Wen, D. S. *Energy Environ. Sci.* **2010**, *3*, 591−600.

(4) Trunov, M. A.; Schoenitz, M.; Dreizin, E. L. *Combust. Theory Modell.* **2006**, *10*, 603−623.

(5) Firmansyah, D. A.; Sullivan, K.; Lee, K. S.; Kim, Y. H.; Zahaf, R.; Zachariah, M. R.; Lee, D. G. *J. Phys. Chem. C* **2012**, *116*, 404−411.

(6) Granier, J. J.; Pantoya, M. L. *Combust. Flame* **2004**, *138*, 373−383.

(7) Huang, Y.; Risha, G. A.; Yang, V.; Yetter, R. A. *Combust. Flame* **2009**, *156*, 5−13.

(8) Rai, A.; Park, K.; Zhou, L.; Zachariah, M. R. *Combust. Theory Modell.* **2006**, *10* (5), 843−859.

(9) Chowdhury, S.; Sullivan, K.; Piekiel, N.; Zhou, L.; Zachariah, M. R. *J. Phys. Chem. C* **2010**, *114*, 9191−9195.

(10) Levitas, V. I.; Asay, B. W.; Son, S. F.; Pantoya, M. *Appl. Phys. Lett.* **2006**, *89*, 071909-1−071909-3.

(11) Levitas, V. I.; Asay, B. W.; Son, S. F.; Pantoya, M. *J. Appl. Phys.* **2007**, *101*, 083524-1−083524-20.

(12) Levitas, V. I.; Pantoya, M. L.; Dikici, B. *Appl. Phys. Lett.* **2008**, *92*, 011921-1−011921-3.

(13) Zhou, L.; Piekiel, N.; Chowdhury, S.; Zachariah, M. R. *Rapid Commun. Mass Spectrom.* **2009**, *23*, 194−202.

(14) Zhou, L.; Piekiel, N.; Chowdhury, S.; Lee, D. G.; Zachariah, M. R. *J. Appl. Phys.* **2009**, *106*, 083306-1−083306-8.

(15) Childs, P. R. N. *Practical Temperature Measurement*; Butterworth Heinemann: London, 2001.

(16) Wimber, R. T.; Halvorson, J. J. *J. Mater.* **1972**, *7*, 564−567.

(17) Hilpert, K. *Rapid Commun. Mass Spectrom.* **1991**, *5*, 175−187.

(18) Deutsch, H.; Hilpert, K.; Becker, K.; Probst, M.; Märk, T. D. *J. Appl. Phys.* **2001**, *89*, 1915-1−1915-7.

(19) Drowart, J.; Chatillon, C.; Hastie, J.; Bonnell, D. *Pure Appl. Chem.* **2005**, *77*, 683−737.

(20) Chervonnyi, A. D. *Russ. J. Inorg. Chem.* **2010**, *55*, 556−559.

(21) Zhou, L.; Piekiel, N.; Chowdhury, S.; Zachariah, M. R. *J. Phys. Chem. C* **2010**, *114*, 14269−14275.

(22) Sullivan, K. T.; Chiou, W. A.; Fiore, R.; Zachariah, M. R. *Appl. Phys. Lett.* **2010**, *97*, 133104-1−133104-3.

(23) Chakraborty, P.; Zachariah, M. R. *Combust. Flame* **2012**, in press.

(24) McHale, J. M.; Auroux, A.; Perrotta, A. J.; Navrotsky, A. *Science* **1997**, *277*, 788−791.

(25) Sullivan, K. T.; Piekiel, N. W.; Wu, C.; Chowdhury, S.; Kelly, S. T.; Hufnagel, T. C.; Fezzaa, K.; Zachariah, M. R. *Combust. Flame* **2012**, *159*, 2−15.

(26) Henz, B. J.; Hawa, T.; Zachariah, M. R. *J. Appl. Phys.* **2010**, *107*, 024901-1−024901-9.

(27) Yuasa, S.; Zhu, Y. X.; Sogo, S. *Combust. Flame* **1997**, *108*, 387−396.

(28) Pangilinan, G. I.; Russell, T. P. *J. Chem. Phys.* **1999**, *111*, 445−448.

(29) Wang, S. F.; Yang, Y. Q.; Sun, Z. Y.; Dlott, D. D. *Chem. Phys. Lett.* **2003**, *368*, 189−194.

(30) Moore, D. S.; Son, S. F.; Asay, B. W. *Propellants, Explos., Pyrotech.* **2004**, *29*, 106−111.

(31) Piehler, T. N.; DeLucia, F. C.; Munson, C. A.; Homan, B. E.; Miziolek, A. W.; McNesby, K. L. *Appl. Opt.* **2005**, *44*, 3654−3660.

(32) Lynch, P.; Fiore, G.; Krier, H.; Glumac, N. *Combust. Sci. Technol.* **2010**, *182*, 842−857.

(33) Goroshin, S.; Mamen, J.; Higgins, A.; Bazyn, T.; Glumac, N.; Krier, H. *Proc. Combust. Inst.* **2007**, *31*, 2011−2019.

(34) Wang, W. Q.; Clark, R.; Nakano, A.; Kalia, R. K.; Vashishta, P. *Appl. Phys. Lett.* **2010**, *96*, 181906-1−181906-3.

(35) Campbell, T. J.; Aral, C.; Ogata, S.; Kalia, R. K.; Nakano, A.; Vashishta, P. *Phys. Rev. B* **2005**, *71*, 205413-1−205413-14.

(36) Puri, P.; Yang, V. *J. Nanopart. Res.* **2010**, *12*, 2989−3002.

(37) Wang, W. Q.; Clark, R.; Nakano, A.; Kalia, R. K.; Vashishta, P. *Appl. Phys. Lett.* **2009**, *95*, 261901-1−261901-3.